

# Vibrational dependence in the dissociative recombination of $O_2^+$

Annemieke Petrigani,<sup>1</sup> Fredrik Hellberg,<sup>2</sup> Richard D Thomas,<sup>2</sup> Mats Larsson,<sup>2</sup> Philip C Cosby<sup>3</sup> and Wim J van der Zande<sup>4</sup>

<sup>1</sup> FOM Institute for Atomic and Molecular Physics, Kruislaan 407, 1098 SJ, Amsterdam, The Netherlands

<sup>2</sup> Molecular Physics, Stockholm University, Albanova University Centre, SE 106 91 Stockholm, Sweden

<sup>3</sup> Molecular Physics Laboratory, SRI International, Menlo Park, CA 94025, USA

<sup>4</sup> Molecule and Laser Physics, IMM, University of Nijmegen, Toernooiveld 1, 6525 ED Nijmegen, The Netherlands

E-mail: a.petrignani@amolf.nl

**Abstract.** We report data on a study into the vibrational dependence in the dissociative recombination of  $O_2^+(X^2\Pi_g)$ . The experiment has been performed with a merged-beam apparatus in the heavy-ion storage ring, CRYRING. We present the total rate coefficients as function of collision energy for five different vibrational populations of the ion beam and the partial rate coefficients and branching fractions near 0 eV collision energy for the vibrational levels  $v = 0, 1$  and  $2$ . Furthermore, we report on the control over and characterization of vibrational populations. The total rate coefficient is found to be weakly dependent on the vibrational excitation. The rate decreases upon increasing vibrational excitation, though only within an order of magnitude. The partial rate coefficients are strongly dependent on the vibrational level; with the  $v = 0$  oxygen ions recombining the fastest. The partial branching fractions are also found to be strongly dependent on the vibrational level, specifically the  $O(^1S)$  quantum yield which increases strongly upon increasing vibrational level.

## 1. Introduction

Dissociative Recombination (DR) is an important reaction for the Earth's atmosphere. It is a sink for low-energy electrons, a source for airglows, and both highly reactive and kinetic product atoms. The DR of  $O_2^+$  is considered to be the only source for the green airglow in the nighttime F-region of our ionosphere. The  $O(^1S)$  and  $O(^1D)$  atoms formed in the DR reaction produce the green and the red airglow, respectively, when relaxing to a lower electronic state. Understanding the DR reaction will enable us to make predictions on airglows and their related variables.

There are numerous previous atmospheric, laboratory and theoretical papers on the DR rate coefficients and branching of  $O_2^+$ . However, the often different vibrational populations present in the studies were not known and, apart from indications of vibrational dependence, no vibrationally resolved cross sections and branching fractions were reported. In spite of these uncertainties the thermal rate is well established. The reported values vary within a factor of two, whereas the ranges of reported  $O(^1S)$  quantum yields differ by an order of magnitude [1]. Although theory is making considerable progress, to the best of our knowledge no complete branching results have been reported for the DR of  $O_2^+$ .

The motivation of the present research is to provide new laboratory answers to the question on the vibrational dependence of the DR reaction. We first discuss the necessary control over the vibrational populations of the parent oxygen ions. Then the total rate coefficients as function of collision energy

**Table 1.** The characterized vibrational populations (in %) of  $O_2^+(X^2\Pi_g, v = 0-5)$  for the ion source settings P1–P5. These are the values used in the fitting of the measured imaging data.

$v$	P1	P2	P3	P4	P5
0	71	60	47	43	29
1	16	22	26	29	30
2	6	9	14	16	22
3	4	5	8	9	10
4	2	3	4	4	5
5	1	1	1	1	4

using ion beams with five different vibrational populations are presented. Finally, we report on the product distributions using these same vibrational populations at 0 eV collision energy, deriving partial (vibrationally resolved) rate coefficients, quantum yields and branching fractions for  $O_2^+(X^2\Pi_g, v = 0-2)$ . These results have recently been published in more detail elsewhere [1].

## 2. Experiment

### 2.1. The ion source

The ion source was constructed at the FOM Institute AMOLF inspired by a similar source at SRI International. It was taken to SRI International for characterization of several vibrational populations using dissociative charge transfer (DCT) reactions between cesium and oxygen [2]. Five different ion-source settings were chosen such that vibrational populations with gradually increasing average excitation were produced (see table 1). An ion-source setting is a set of conditions that influence the formation and quenching of the ions before they exit the ion source [1]. After the characterization, the ion source was shipped to the Manne Siegbahn Institute and integrated into the heavy ion storage ring, CRYRING. The populations were then reproduced by switching back to their corresponding ion-source settings and for each ion-beam population the DR rate as function of collision energy together with the product distributions at 0 eV collision energy were investigated.

### 2.2. The DR experiment

The DR experiment was carried out in a merged-beams apparatus at CRYRING. The ions were accelerated in 1.1 s to a full beam energy of 3.05 MeV after which they were allowed to coast in the ring. During each revolution, the ions are merged with an electron beam in the so-called electron cooler. The electron cooler has a length of 0.85 m and the total circumference of the storage ring is 51.6 m. The ion beam passes through the electron cooler many times during its storage time. The cooler acts as the site for the DR reactions. Other possible interactions in the merged beam section are elastic and super-elastic collisions (SECs) between the ions and the electrons [3, 4]. The SECs may cool the vibrational populations significantly and in order to investigate these collisions or any other time dependent factor, like the product vibrational states arising from the decaying metastable  $O_2^+(a^4\Pi_u)$  ions, data was taken at two different storage times. There are also dissociative charge transfer reactions [5] between the ions and rest gas molecules occurring throughout the ring. These charge transfer reactions produce two neutral product atoms, as in DR, and therefore constitute a background signal which must be accounted for. More details on the CRYRING can be found elsewhere in the literature [5, 6].

In the first part of the DR experiment the reaction rate for each of the ion-source settings was measured as function of the collision energy up to 0.4 eV. A surface barrier detector situated in the zero-degree arm following the electron cooler was used to detect the neutral atoms produced in the DR reaction [5]. Measurements were taken during the full storage time. The collision energy was ramped between 0 eV and 0.4 eV by both accelerating and decelerating the electron beam with respect to the ion beam, ensuring that a collision energy of 0 eV is achieved. This ramp was set between 2.25 and 3.75 s storage time. The count rate due to background reactions was measured independently for each population by turning the

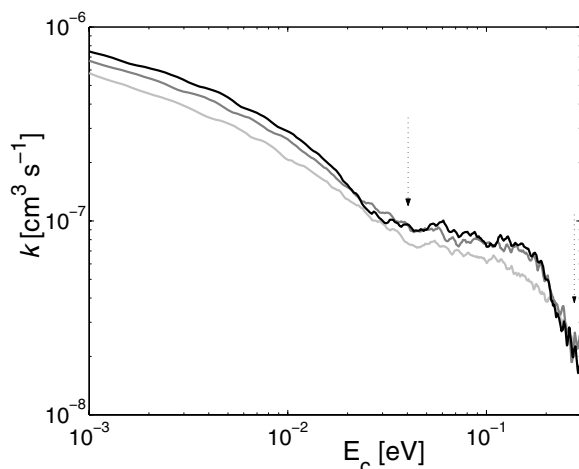


**Figure 1.** The total rate coefficient  $k$  as function of collision energy  $E_c$  up to 0.3 eV on a bi-logarithmic scale. The black solid rate curve corresponds to the coldest population P1, the dark grey curve to the intermediate population P3 and the light grey curve to the hottest population P5. The arrows indicate the local minima in the curves.

collision energy briefly up to 5 eV. Background subtraction, normalization to the beam decay and all the necessary corrections [7–9] were taken into consideration to determine the total rate coefficient  $k$ .

In the second part of the DR experiment, the DR dynamics were investigated while restricting the collision energy to a nominal 0 eV (there is a 2 meV electron transverse temperature to consider). The fragment atoms produced in DR events were detected with a stack of MCP plates, followed by a phosphor plate and a CCD camera [10], which recorded only the position of the fragments. The imaging spectrum acquired for each vibrational population is therefore a superposition of 2D distance distributions for each vibrational level present in the ion beam, weighted by their relative partial cross sections and their partial branching fractions. The background contribution was again measured separately for each of the ion-source settings, this time by turning the electrons off. Data from both the DR and the background reactions were collected during the full storage time. In addition, each event was labelled with a time stamp relative to the start of a measuring cycle in time increments of 50 ms. The fitting procedure generates a distance distribution for each  $O_2^+(v)$  state dissociating into the four open dissociation limits. The dissociation towards  $O(^3P) + O(^1S)$  has not been included since both experimental and theoretical research indicate it will not contribute [1]. Furthermore, in fitting the distance spectra, it has been assumed that the DR reaction is isotropic and a 300 K rotational distribution, the finite interaction length, and the projection of the total distance onto the 2D detector were all taken into account. Finally, the relative partial cross section and the partial branching fractions for each vibrational state were assumed to be independent of the rotational state.

### 3. Results

#### 3.1. The total rate coefficient

The measured total rate coefficients for the five vibrational populations P1–P5 (see table 1) have been obtained as function of electron energy. The rate coefficient curves of P1 (coolest), P3 and P5 (hottest) are shown in figure 1. The error bars (not shown) in the curves are mainly determined by statistics, and become significant above 100 meV. We observe that the total rate coefficient decreases upon increasing vibrational excitation near 0 eV collision energy. This observation suggests that the cross section for  $O_2^+(v=0)$  is higher than that of  $v=1$ . The observed rates vary within a factor of two, which is consistent with the small range of thermal rates already reported [1]. The general behavior of the rate coefficient due to the direct DR process is proportional to the inverse square root of the collision energy. Therefore, multiplying the rate by the square root of the collision energy will reveal the resonant features as oscillations around a collision-energy independent level (see figure 2) The resonances are indicated with arrows. The rate for the coolest population P1 shows a strong variation from the purely  $1/\sqrt{E_c}$  behavior. However, upon increasing excitation the curves become flatter and the resonant features are virtually absent for the hottest population P5. Further analysis can be found elsewhere [1].

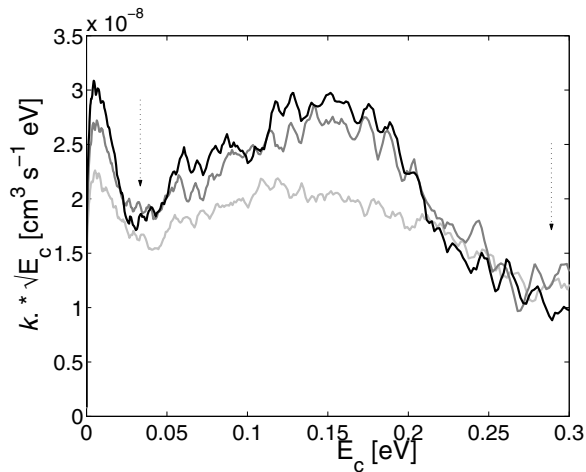


**Figure 2.** The total rate coefficients multiplied by the square root of the collision energy on a bilinear scale, revealing the resonant features as oscillation around a collision-energy independent level. The black solid rate curve corresponds to the coldest population P1, the dark grey curve to the intermediate population P3 and the light grey curve to the hottest population P5. The arrows indicate the local minima in the curves, as in figure 1.

### 3.2. The partial rate coefficients and branching fractions

Figure 3 shows two distance distributions as measured with the imaging technique. The black symbols correspond to the coolest and the grey symbols to the hottest population. The difference in the peak widths shows the difference in the vibrational excitation, with the broader peak indeed corresponding to the hotter population. The difference in relative peak heights is an indication that the partial cross sections and/or partial branching fractions are vibrational dependent. In the fitting procedure, all the product distributions obtained for populations P2–P5 were fitted considering  $v = 0–5$ , while simultaneously optimizing the partial cross section and partial branching fractions for each vibrational level. The product distributions obtained for P1 were fitted separately only taking into account the first four vibrational levels,  $v = 0–3$ . The latter fit serves as a consistency check for the simultaneous fit of P2–P5. We investigated two storage times to estimate the systematic errors introduced by the omission of the SECs and the decaying electronically excited metastable state [1]. These systematic errors were highest for the sparsely populated higher vibrational levels and we therefore present the results for the vibrational levels  $v = 0, 1$  and 2 only.

The relative partial branching fractions and partial cross sections  $\sigma_v$  for  $v = 0–2$  at storage time 2.5–4.0 s from the simultaneous fit of P2–P5 are given in table 2. The partial cross sections are relative to  $\sigma_0$ , the cross section obtained for  $v = 0$ . The partial branching fractions and cross sections are strongly dependent on the vibrational state. The cross section for  $v = 0$  is the highest and the  $O(^1S)$  yield increases considerably upon increasing vibration. Further analysis can be found elsewhere [1].

## 4. Conclusions

In summary, the present research gives further and more detailed insights in the vibrational dependence of the DR of  $O_2^+$ . It has provided partial cross sections and partial branching fractions for  $v = 0–2$  together with total rate coefficients for five different vibrational populations. The partial branching fractions and

**Table 2.** The partial cross sections  $\sigma_v$  (relative to  $\sigma_0$ ) and branching fractions (in %) for  $O_2^+(X^2\Pi_g, v = 0–2)$  resulting from the simultaneous fit of the P2–P5 imaging spectra at storage time 2.5–4.0 s.

$v$	$\sigma_v$	$O(^1D)+O(^1S)$	$O(^1D)+O(^1D)$	$O(^3P)+O(^1D)$	$O(^3P)+O(^3P)$
0	1	$5.8 \pm 0.5$	$20.4 \pm 0.3$	$47.3 \pm 0.8$	$26.5 \pm 0.8$
1	$0.31 \pm 0.13$	$13.9 \pm 3.1$	$51.0 \pm 5.4$	$27.8 \pm 5.1$	$7.3 \pm 7.5$
2	$0.52 \pm 0.16$	$21.1 \pm 2.5$	$2.5 \pm 2.1$	$76.4 \pm 2.2$	$0.02 \pm 0.03$

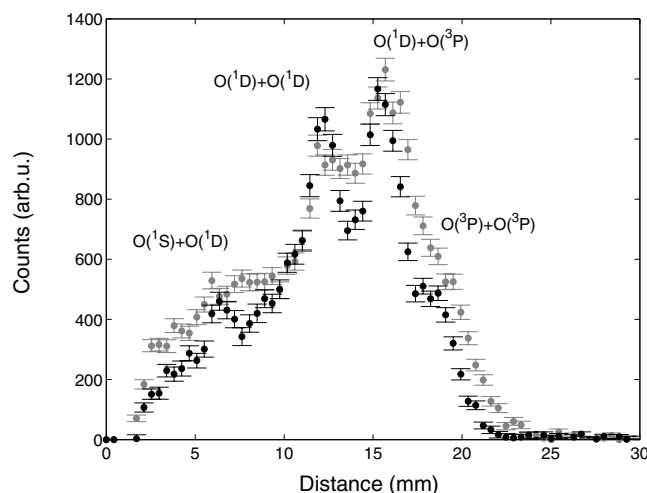


**Figure 3.** The product distributions of the coolest and the hottest vibrational population P1 (black) and P5 (grey), respectively at storage time 2.5–4.0 s.

the partial cross sections are strongly dependent on the vibrational level of the parent ion, with the  $O(^1S)$  yield increasing substantially upon increasing vibrational level. The partial cross sections agree with the total cross sections measured, which also indicate the  $v = 0$  rate to be fastest. The weak dependence of the total rate coefficients on the vibrational population is consistent with the small range of thermal rates previously reported. It also excludes vibrational specific rates that differ by an order of magnitude. The present results may be extended to higher vibrational levels once SECs can be modelled and the production of the metastable state avoided.

### Acknowledgments

This work is part of the research program of the "Stichting voor Fundamenteel Onderzoek der Materie (FOM)", which is financially supported by the "Nederlandse organisatie voor Wetenschappelijk Onderzoek (NWO)". It has been partially supported by the NASA Planetary Atmospheres Program under grant NAG5-11173 to SRI International. Support has also been given by the EU research-training network Electron Transfer Reactions (ETR) under HPRN-CT-2000-00142. We thank the staff of the Manne Siegbahn Laboratory for their part in making the experiments possible.

### References

- [1] Petrigani A, Cosby PC, Hellberg F, Thomas RD, Larsson M and van der Zande WJ 2005 Vibrationally resolved rate coefficients and branching fractions in the dissociative recombination of  $O_2^+$  *J. Chem. Phys.* **122** 014302
- [2] Walter C W, Cosby PC and Peterson JR 1993 Rovibrational product distributions of  $O_2^+$  from the reaction of  $O^+(^4S)$  with  $CO_2$  *J. Chem. Phys.* **98** 2860
- [3] Krohn S, Amitay Z, Baer A, Zajfman D, Lange M, Knoll L, Levin J, Schwalm D, Wester R and Wolf A 2000 Electron-induced vibrational deexcitation of  $H_2^+$  *Phys. Rev. A* **62** 032713
- [4] Zajfman D, Krohn S, Lange M, Kreckel H, Lammich L, Strasser D, Schwalm D, Urbain X and Wolf A 2003 Physics with molecular ions in storage rings *Nucl. Instrum. Methods B* **205** 360
- [5] Peverall E *et al.* 2001 Dissociative recombination and excitation of  $O_2^+$ : Cross sections, product yields and implications for studies of ionospheric airglows *J. Chem. Phys.* **114** 6679
- [6] Larsson M 1997 Dissociative recombination with ion storage rings *Annu. Rev. Phys. Chem.* **48** 151
- [7] Al-Khalili A *et al.* Absolute high-resolution rate coefficients for dissociative recombination of electrons with  $HD^+$ : Comparison of results from three heavy-ion storage rings *Phys. Rev. A* **68** 042702
- [8] N ag ard MB *et al.* 2002 Dissociative recombination of  $D^+(D_2O)_2$  water cluster ions with free electrons *J. Chem. Phys.* **117** 5264
- [9] Neau A *et al.* 2000 Dissociative recombination of  $D_3O^+$  and  $H_3O^+$ : Absolute cross sections and branching ratios *J. Chem. Phys.* **113** 1762
- [10] Hellberg F, Petrigani A, van der Zande WJ, Ros en D, Thomas RD, Neau A and Larsson M 2003 Dissociative recombination of  $NO^+$ : Dynamics of the  $X^1\Sigma^+$  and  $a^3\Sigma^+$  electronic states *J. Chem. Phys.* **118** 6250